Proceedings World Geothermal Congress 2026
Calgary, Canada, June 8 – 11, 2026

Effectiveness of Integrating Lineament and Fluid Geochemistry Data for 'Steam Spot' Detection with Verification by Shallow Drilling

Katsuaki Koike[1*], Taiki Kubo[1], Koki Kashiwaya[1], Brenda A. Kusumasari[1], Tada-nori Goto[2], Sudarto Notosiswoyo[3], Mohamad Nur Heriawan[3], Irwan Iskandar[3], Asep Saepuloh[4], Arie Naftali Hawu Hede[3], Nenny Miryani Saptadji[3] and Sutopo[3]

Graduate School of Engineering, Kyoto University[1*], Graduate School of Science, University of Hyogo[2], Faculty of Mining and Petroleum Engineering, Bandung Institute of Technology[3], Faculty of Earth Sciences and Technology, Bandung Institute of Technology [4]

koike.katsuaki.5x@kyoto-u.ac.jpi

Keywords: Data integration, fracture system, radon concentration, water geochemistry, Patuha

ABSTRACT

To detect locations suitable to set production wells and increase the success ratio of production wells to reach fluid and steam-rich fracture zones, this study aims to develop a method of specifying 'steam spot' by targeting the Patuha geothermal field (PGF) in Indonesia. 'Steam spot' means a permeable fracture zone acting as a main path of hydrothermal fluid that enables large and long-term power generation. A potential map of steam spot existence is produced by integrating the datasets of lineament density, ^{222}Rn concentration in soil gas, and specific element and component concentrations in water samples. Characterization and verification of the generated potential map are implemented by comparing fluid geochemical features and 3D resistivity models and additionally, temperature logging data and homogenization temperatures of fluid inclusions by shallow drilling at selected sites with different potential values. Effectiveness of the proposed method of steam-spot potential mapping is demonstrated through the comparisons.

1 INTRODUCTION

Towards large increase in geothermal power generation, one of the most important subjects is accurate positioning of production wells by reducing exploration drilling costs. For this challenge, we aim to develop a method of specifying 'steam spot' for suitable location of production wells by targeting the Patuha geothermal field (PGF) in Indonesia. PGF is one of the representative Indonesian areas rich in geothermal resources with the operating geothermal power plant. 'Steam spot' defined by Koike et al. (2021) means a permeable fracture zone acting as a main path of hydrothermal fluid that enables large and long-term power generation. The steam-spot detection is founded on an integration of multiple datasets related to fracture system, concentration of an effective component of soil gas, and geochemical features of fluid. For preparing the datasets, lineament analysis, repeated measurements of radon concentration at multiple sites, and composition and isotope analyses of water samples were implemented. Resultant potential map of steam spot existence is verified through comparisons with 3D resistivity models and, at selected sites with different potential values, temperature logging data and homogenization temperatures of fluid inclusions by shallow drilling.

2 STUDY AREA AND METHODS

2.1 Outline of the PGF

Details of the geological setting and geothermal features of the PGF are described in Rahayudin et al. (2020). Only their outline is summarized below. The PGF is located in West Java, Indonesia and southwest of the Bandung Basin (Fig. 1a) with thirteen production wells over a 35 km^2 area. A feature of the PGF is presence of a vapor-dominated or two-phase reservoir at a depth of 1 km. Thickness of the hot vapor-dominated layer was estimated to be about 0.5 km with 200 to 240 °C by several deep-well investigations. The PGF consists mainly of late Pliocene to Quaternary pyroclastic and andesitic lavas above the basement, Tertiary volcanic rocks, with an active volcano, Mt. Patuha, in the middle. There are many geothermal manifestations such as fumaroles, hot springs, mud pools, hydrothermal alteration zones, and craters. Among them, the crater lake Kawah Putih is the most remarkable accompanying many fumaroles, alteration minerals, and acidic water on southern Mt. Patuha (Fig. 1). The manifestations distribution is controlled mainly by the NW–SE and NE–SW normal faults.

2.2 Lineament Extraction

Lineament is a linear or slightly curved topographic pattern appeared on remotely sensed and DEM (Digital

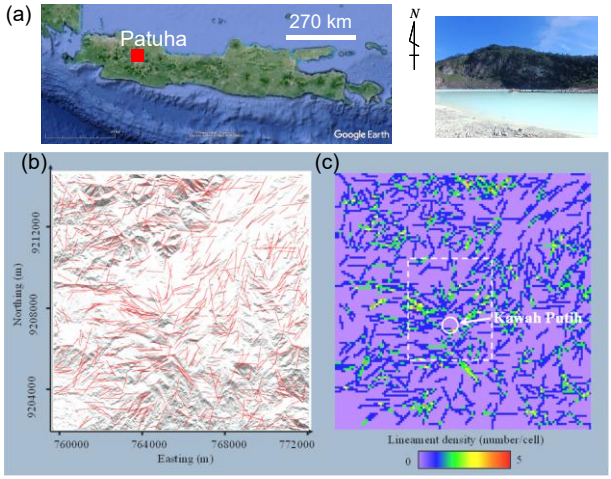


Figure 1. Location of the study area, Patuha geothermal field in West Java, Indonesia with the most remarkable geothermal manifestation, crater lake Kawah Putih (a), extracted lineament distribution overlapped with the multi-shaded LiDAR-DEM image (b), and lineament density map (c).

Elevation Model) imagery. Most of lineaments correspond to fracture-caused topographic features such as a long straight valley by selectively eroded fracture zone. To characterize the regional fracture system in the PGF, a lineament analysis using a precise DEM was implemented. The DEM was produced by an airborne LiDAR survey covering an area of 12 km by 12 km with the spatial resolution 1 m. A multi-shading technique that illuminates DEM from several directions was applied to the DEM to reduce the illumination effect from a light source, and linear features were extracted by an improved version of the Segment Tracing Algorithm (STA; Koike et al., 1995). Two linear features with similar directions and short distance between the starting point of one feature and the ending point of the other feature were grouped into one longer feature, and this grouping processing was repeated for all the linear features. The resultant grouped linear features were defined as lineaments. Using the extracted lineaments, a lineament density map was prepared by gridding the DEM area with a unit cell of 100 m by 100 m size, in which the density was defined by the number of lineaments passing through each cell.

2.3 Radon Survey

^{222}Rn is the longest half-life, 3.823 days, among the radon isotopes. Effectiveness of ^{222}Rn concentration in soil gas for estimating reservoir temperature and detecting permeable factures along which geothermal fluids ascend from deep portions with large volume and velocity was demonstrated by Koike et al. (2014) by a case study in an active volcano area. RAD7 (Durridge Company, Inc.) was used to measure the ^{222}Rn concentration (Bq/m^3) in soil gas. For the gas sampling, a borehole was dug down to about a depth of 1 to 2 m and protected by a polyvinyl chloride pipe with 1.75 inches diameter and a rubber stopper on the top. In total 17 borehole sites were placed near the manifestations and fault intersections, and the ^{222}Rn concentrations at each site were repeatedly measured at approximately fixed intervals from July to December 2020. One cycle measurement takes 5 minutes. To increase the data reliability, measurements were repeated by four or more cycles. As a result, five to ten concentration data were obtained at each site.

2.4 Geochemical Analyses of Water and Rock Samples

By targeting hot and cold springs, water samples were collected from 16 sites, and concentrations of major ions and trace elements were measured by methods of ion chromatography and ICP-MS. To specify the fluid origin of the PGF, water stable isotopes, δD and δ^{18}O, were also measured. The ion and element concentrations with partial pressures of the non-condensable gases were used for a multicomponent geothermometer to estimate the reservoir temperature through the iGeoT code (Reed and Spycher, 1984). By those geochemical factors, the equilibrium condition is optimized under an assumed mineral assemblage and a mineral saturation index. The mineral assemblage, i.e., the composition of main minerals, was determined by XRD analyses of rock samples.

2.5 TEM and MT Surveys for Resistivity Modeling

To verify high potential zones of steam spot existence, Transient Electro-Magnetic (TEM) and magnetotelluric (MT) surveys were adopted to reveal detailed resistivity distribution in the shallow depth range down to a depth of about 100 m by TEM and regional distribution in the wide depth range down to a depth of about 3 km by MT. The resistivity tends to be low in high liquid content zones and advanced hydrothermal alteration zones mainly composed of clay minerals. Two resistivity models with different depth ranges were constructed by an inversion

analysis of measured TEM and MT apparent resistivity data in the configured frequency ranges.

3 RESULTS

3.1 Extracted Lineaments and Lineament Density Map

The multi-shaded LiDAR-DEM image, which was changed to 10-m resolution, is shown in Figure 1b with the extracted lineaments by the STA. In this precise image, topographic features such as valleys and the crater lake Kawah Putih appear clearly. Obviously, lineaments trending NNE-SSW to NE-SW and NNW-SSE to NW-SE are dominant, which corresponds to the main fault directions. This directional trend can be expressed more clearly by the lineament density map (Fig. 1c). Relatively large densities colored by green to red are distributed along two directions, NE-SW and NW-SE. It is noted that Kawah Putih is situated at an intersection of the two high density rows in those directions, which suggests a formation of ascent path of fluids by the fracturing. Another feature is that the more high-density zones are distributed in the north part than the south part, and such zones are confirmed to correspond to concentrated zones of the hot springs in the north part.

3.2 ^{222}Rn Concentrations and Temporal Change Feature

The concentration at three cycles was selected as a representative value at each borehole site, because the concentration took the maximum mostly common to the sites. The resultant ^{222}Rn concentrations at all the sites are shown in Figure 2a. Similar to the feature of lineament density, sites of relatively high ^{222}Rn concentrations colored by green to red tend to be distributed in the north part. The temporal changes in the ^{222}Rn concentrations at the highest concentration site (TTN-03) and a medium concentration site (TTN-14) are compared in Figure 2b. A noted concentration feature of TTN-03 is the large increase from the first to third cycle and the maintenance of the high concentration despite the long-elapsed time. Contrary to it, increase in the concentrations at TTN-14 is small. This different pattern is caused by the volume and velocity of carrier gas of ^{222}Rn, as interpreted by Koike et al. (2024), i.e., constant gas supply with large volume and high velocity probably occurs from deep portions at the high concentration site as TTN-14. Such gas supply is possible in a permeable path for fluid ascent.

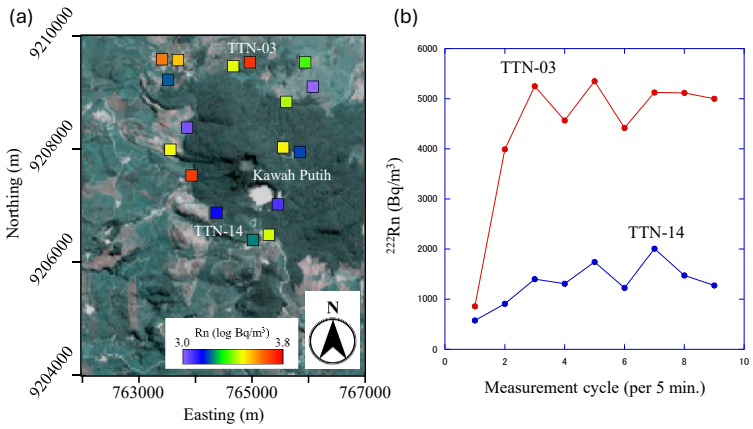


Figure 2. Distribution of the ^{222}Rn concentration at each borehole site (a) and comparison of temporal concentration changes between the highest site (TTN-03) and a medium site (TTN-14) (b).

3.3 Fluid Characterization through Geochemical Data

Among the 16 sites, δD and δ^{18}O data at 14 sites were plotted around and on the meteoric water line (WMWL). The other two sites are crate lake waters including Kawah Putih in which magmatic water is certainly mixed with meteoric water. Consequently, the main fluid origin in the PGF can be interpreted to be meteoric water. In addition, clustering analysis of the measured δD and δ^{18}O and concentrations of the major ions, trace metal elements, and REE was adopted for the 16 sites data by the Ward's method, aiming at zoning the sampling sites based on the similarity of geochemical features. As a result, the 16 sites were clearly divided into two zones, the sites in the north and south parts. The south part is generally characterized by the low concentrations of major cations, low pH, and high concentrations of SO_4^{2-}, Cl^-, Al, and Fe. Meanwhile, major cations are relatively rich, and Al and Fe concentrations are low in the north part. Therefore, the fluids in the south and north parts are interpreted as acidic condensed water and neutral HCO_3 type groundwater, respectively, and both are heated by the magma-originated steam.

3.4 Potential Mapping of Steam Spot Existence

The datasets of lineament density, the ^{222}Rn concentration in soil gas at each site, and concentrations of Al and SO_4 in the water samples were used and integrated for potential mapping of steam spot existence over an area of 5 km E–W by 4 km N–S. This target area is shown by the white rectangle of the dashed line in Figure 1c, and those concentration data were log-transformed to reduce the bias in their distributions. Because the ^{222}Rn, Al, and SO_4 concentrations were point data at sites, they were interpolated by a geostatistical method, ordinary kriging or inverse-distance weighted method and changed to 2D distributions with the same unit cell size and grid system as those of the lineament density. Each dataset was normalized into the range from 0 (the minimum value) to 1 (the maximum value). Referring to a previous potential mapping of steam spot existence by Koike et al. (2021), Al and SO_4 were selected as the effective chemical parameters that are thought to be strongly correlated with hydrothermal fluids from deep portions and affected by mixture rate with the fluids. The potential was evaluated by adding or subtracting the four indices simply with equal weight. Subtraction was adopted for the SO_4 concentration, because the SO_4 concentrations in the water samples from production wells were generally lower than those from hot and cold springs in the case study of Koike et al. (2021).

The resultant potential map is exhibited in Figure 3a, which highlights that relatively high potential zones are concentrated in the middle area in the north part and limited around Kawah Putih in the south. Accordingly, the PGF can be characterized by the separation of two zones, relatively high potential in the north part and low potential in the south part. This separation corresponds to the grouping of geochemical features of the water samples as above-mentioned. To verify the evaluated potential values, two sites for drilling temperature core hole, TCH-A and B, were selected in middle and high potential zones, respectively (Fig. 3a).

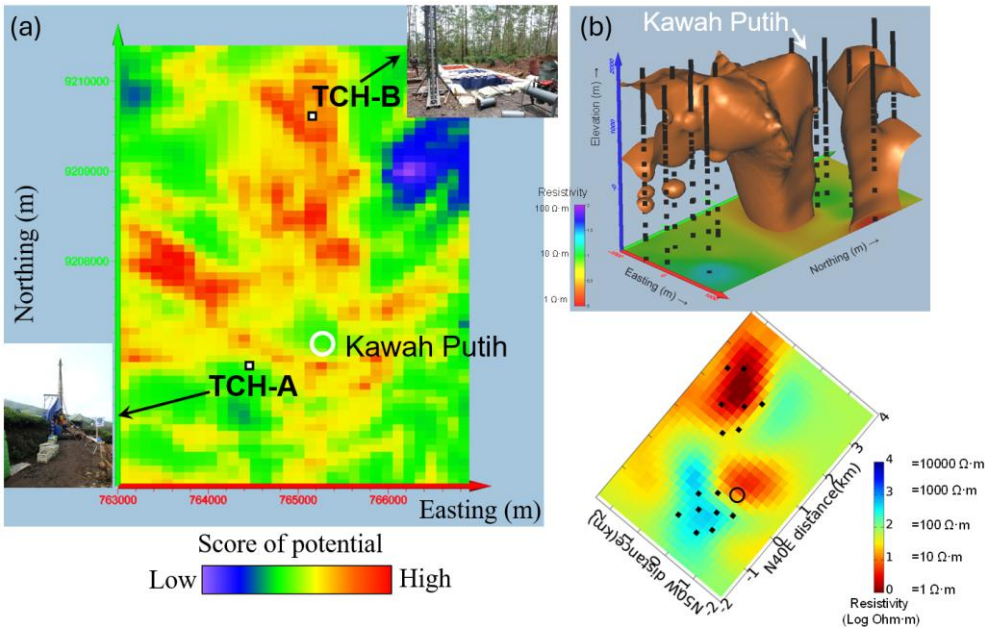


Figure 3. Potential map of steam spot existence by integrating four parameters with photos of two temperature core hole sites, TCH-A and B (a), perspective view of particularly low MT resistivity zones less than 3 Ω·m (b), and a horizontal cross-section of MT resistivity model at a depth of 1400 m (c).

4 DISCUSSIONS

4.1 Confirmation of Alteration Zone Extent by TEM and MT Resistivity Models

Through an inversion analysis of the MT data obtained at 15 sites, a 3D resistivity distribution model was produced. Particularly low resistivity zones less than 3 Ω·m are chosen from this model and displayed perspectively in Figure 3b. Such a particularly conductive feature probably originates from developments of hydrothermal alteration zones with high contents of fluids and clay minerals. Two wide alteration zones developed horizontally with vertical continuity around Kawah Putih are conspicuous, which may indicate the horizontal extent of caprocks and the formation of ascent paths of hydrothermal fluids. Two reservoirs may have formed under these caprocks. From a horizontal cross-section at a depth of 1400 m, extremely low resistivity zone close to 1 Ω·m can be confirmed to extend only in the north part (Fig. 3c), which suggests a more development of the hydrothermal alteration zone by higher geothermal activity in the north part. This feature corresponds to the more high potential zones of steam spot existence in the north part. The TEM results also suggest the development of hydrothermal alteration zones below a depth of 30 m at both the TCH-A and B sites by the low resistivity less than 10 Ω·m.

4.2 Confirmation of Higher Potential by Temperature Logging and Homogenization Temperature

The TCH-A and B were drilled vertically down to depths of 303 m and 203.5 m, respectively. At the same depth of 200 m, the temperatures were TCH-A: 21.3 °C and TCH-B: 31.8 °C. The temperature gradient changed abruptly at a depth of 185 m and increased below it at TCH-B, whereas almost the same temperatures continued downward at TCH-A. Therefore, high temperature in the deep portions is estimated at the TCH-B site.

The drill cores were mostly composed of andesite common to the two sites, but conspicuous minerals identified by XRD were slightly different as TCH-A: albite, andesine, and chlorite versus TCH-B: anorthite, kaolinite, andesine, and cristobalite. Using fluid inclusions in quartz, homogenization temperatures and salinities were measured, and 273 data in total were obtained from 20 cores in the ranges from 145 to 268 °C and from 3.2 to 10.8 (wt% NaCl equivalent). The mean homogenization temperatures and salinities were TCH-A (75 data): 165 °C–4.8 wt% and TCH-B (198 data): 242 °C–8.5 wt%. Higher temperature at TCH-B agrees with the trend of temperature logging data and roughly matches the estimated reservoir temperature, 245 °C, using the water samples through a multicomponent geothermometry (Kusumasari et al., 2024). Consequently, corresponding to the potential mapping result, higher potential of steam spot existence at the TCH-B site with a higher reservoir temperature is plausible, and the middle area in the north part of PGF with the high potential values is regarded to be suitable to set production wells.

5 CONCLUSION

To detect locations suitable to set production wells, this study deepened a concept of steam spot and proposed a potential mapping method of steam spot existence by selecting the PGF, Indonesia as a case study target. The potential map was produced by integrating the datasets of lineament density, ^{222}Rn concentration in soil gas, and concentrations of Al and SO_4 in the water samples. The resultant map highlighted the separation of PGF into two zones, relatively high and low potential in the north and south parts, respectively, which corresponded to the grouping of fluid geochemical features. The validity of high potential in the north part was confirmed by an extent of the extremely low MT resistivity there, which may express a well-developed hydrothermal alteration zone. Furthermore, two TCHs were drilled at middle and high potential sites, and both the temperature by well logging and homogenization temperature by fluid inclusion analyses using the cores were higher at the higher potential site. Through these correspondences, the effectiveness of the proposed method of steam-spot potential mapping was demonstrated consequently, which may contribute to increasing the success ratio of production wells to reach fluid and steam-rich fracture zones.

Acknowledgements

This study was supported by the Japan Science and Technology (JST) and Japan Society for the Promotion of Science (JSPS) in collaboration with Kyoto University, Bandung Institute of Technology, and Indonesian and Japanese companies through the aXis (Grant No. JPMJAS2003) and KAKENHI (Grant No. 21KK0090) projects.

REFERENCES

Koike, K., Nagano, S., and Ohmi, M.: Lineament Analysis of Satellite Images Using A Segment Tracing Algorithm (STA), *Computers & Geosciences*, **21**, (1995), 1091–1104.

Koike, K., Yoshinaga, T., and Asaue, H.: Characterizing Long-Term Radon Concentration Changes in A Geothermal Area for Correlation with Volcanic Earthquakes and Reservoir Temperatures, *Journal of Volcanology and Geothermal Research*, **275**, (2014), 85–102.

Koike, K., Kubo, T., Kashiwaya. K., Tada, Y. Goto, T.-N., Sakurai, S., Notosiswoyo, S., Heriawan, M.N., lskandar, I., Saepuloh, A., Hawu Hede, A.N., Saptadji, N.M., and Sutopo: Technology Development of 'Steam Spot' Detection for Suitable Location of Production Wells by Integrating Geoscientific Methods, *Proceedings*, World Geothermal Congress 2020+1, Reykjavik, Iceland (2021).

Kusumasari, B.A., Kashiwaya, K., Tada, Y., Rahayudin, Y., Koike. K.: Reservoir Temperature Assessment by Multicomponent Geothermometry through A Case Study of Patuha Geothermal Field, Indonesia, *IOP Conf. Series: Earth and Environmental Science*, **1383**, (2024), 012007.

Rahayudin, Y., Kashiwaya, K., Tada, Y., Iskandar, I., Koike, K., Atmaja, R.W., and Herdianita, N.R.: On the Origin and Evolution of Geothermal fluids in The Patuha Geothermal Field, Indonesia Based on Geochemical and Stable Isotope Data, *Applied Geochemistry*, **114**, (2020), 104530.

Reed, M.H., and Spycher, N.F.: Calculation of pH and Mineral Equilibria in Hydrothermal Waters with Application to Geothermometry and Studies of Boiling and Dilution, *Geochimica et Cosmochimica Acta*, **48**, (1984), 1479–1492.